



Elevated methylmercury in Antarctic surface seawater: The role of phytoplankton mass and sea ice



Fange Yue^a, Yanbin Li^{b,c}, Yanxu Zhang^d, Longquan Wang^a, Dan Li^e, Peipei Wu^d, Hongwei Liu^a, Lijin Lin^f, Dong Li^g, Ji Hu^g, Zhouqing Xie^{a,*}

^a Institute of Polar Environment & Anhui Key Laboratory of Polar Environment and Global Change, Department of Environmental Science and Engineering, University of Science and Technology of China, Hefei, Anhui 230026, China

^b Frontiers Science Center for Deep Ocean Multispheres and Earth System, and Key Laboratory of Marine Chemistry Theory and Technology, Ministry of Education, Ocean University of China, Qingdao 266100, China

^c College of Chemistry and Chemical Engineering, Ocean University of China, Qingdao 266100, China

^d School of Atmospheric Sciences, Nanjing University, Nanjing, Jiangsu 210023, China

^e College of Environmental Science and Engineering, Ocean University of China, Qingdao 266100, China

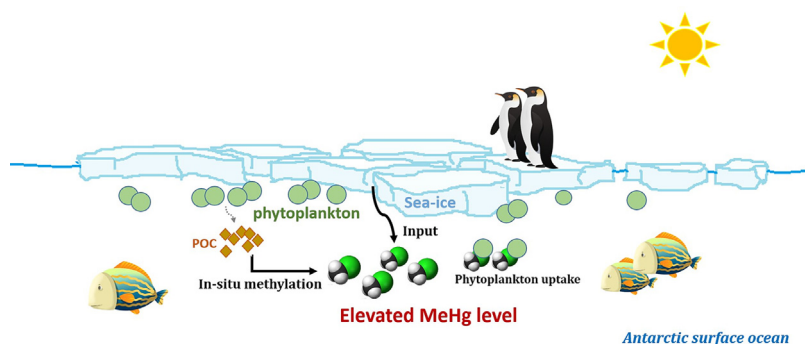
^f College of Oceanic and Atmospheric Sciences, Ocean University of China, Qingdao 266100, China

^g Second Institute of Oceanography, Ministry of Natural Resources (MNR), Hangzhou 310000, China

HIGHLIGHTS

- Deep vertical profiles (up to 4000 m) of MeHg_T in Antarctic marginal seas were explored.
- High MeHg_T concentrations in oxic surface seawater (upper 50 m depth) in Antarctica were found.
- Hg methylation facilitated by phytoplankton may be important for the elevated MeHg_T in Antarctic surface seawater.
- The presence of sea-ice may facilitate MeHg_T elevation in Antarctic surface seawater.

GRAPHICAL ABSTRACT



ARTICLE INFO

Editor: Xinbin Feng

Keywords:

Methylmercury
Southern Ocean
Water mass
Methylation
Phytoplankton
Sea ice

ABSTRACT

Methylmercury is a neurotoxin that is biomagnified in marine food webs. Its distribution and biogeochemical cycle in Antarctic seas are still poorly understood due to scarce studies. Here, we report the total methylmercury profiles (up to 4000 m) in unfiltered seawater (MeHg_T) from the Ross Sea to the Amundsen Sea. We found high MeHg_T levels in oxic unfiltered surface seawater (upper 50 m depth) in these regions. It was characterized by an obviously higher maximum concentration level of MeHg_T (up to 0.44 pmol/L, at a depth of 3.35 m), which is higher than other open seas (including the Arctic Ocean, the North Pacific Ocean and the equatorial Pacific), and a high MeHg_T average concentration in the summer surface water (SSW, 0.16 ± 0.12 pmol/L). Further analyses suggest that the high phytoplankton mass and sea-ice fraction are important drivers of the high MeHg_T level that we observed in the surface water. For the influence of phytoplankton, the model simulation showed that the uptake of MeHg by phytoplankton would not fully explain the high levels of MeHg_T, and we speculated that high phytoplankton mass may emit more particulate organic matter as microenvironments that can sustain Hg in-situ methylation by microorganisms. The presence of sea-ice may not only harbor a microbial source of MeHg to surface water but also trigger increased phytoplankton mass, facilitating elevation of MeHg in surface seawater. This study provides insight into the mechanisms that impact the content and distribution of MeHg_T in the Southern Ocean.

* Corresponding author.

E-mail address: zqxie@ustc.edu.cn (Z. Xie).

1. Introduction

Mercury (Hg) is a global pollutant that can be transported over long distances through atmospheric circulation and deposited in terrestrial and aquatic ecosystems (Ariya et al., 2015; Driscoll et al., 2013; Yue et al., 2022). Methylated mercury (MeHg, including monomethylmercury [CH_3Hg] and dimethylmercury [$(\text{CH}_3)_2\text{Hg}$]) has the highest toxicity among Hg compounds (Andreoli and Sprovieri, 2017; Roman Henry et al., 2011). As a neurotoxin, CH_3Hg can enter organisms through intestinal absorption and travel through the blood to organs and tissue, poisoning the central nervous system and causing irreversible damage to the cerebrum and cerebellum (Clarkson and Magos, 2006). In addition, CH_3Hg tends to be biomagnified in the aquatic food web. The CH_3Hg level in predatory fish was found to be 10^6 – 10^7 times higher than the level of CH_3Hg detected in the water body (McMeans et al., 2015; Wu et al., 2019), which demonstrates the potential exposure risks of MeHg toward apex predators (Beckers and Rinklebe, 2017).

The MeHg concentrations measured from world oceans generally present a distinct vertical profile within the water column. The maxima are usually observed in subsurface waters (with a general depth of approximately 100–500 m) with low dissolved oxygen (DO), where heterotrophic microorganisms metabolize and decompose sinking organic matter (OM) (Bratkic et al., 2016; Cossa et al., 2011; Kim et al., 2017; Wang et al., 2012). This suggests an association between Hg methylation and heterotrophic OM remineralization. It has been suggested that anaerobic microbes such as iron- and sulfate-reducing bacteria play key roles in Hg methylation in aquatic environments (Driscoll et al., 2013). Further studies revealed that the *hgcA* and *hgcB* genes and their encoding proteins are responsible for anaerobic microbial Hg methylation (Parks Jerry et al., 2013). However, known anaerobic Hg methylators are unlikely to thrive and produce MeHg in oxic marine waters since anoxic conditions are rarely reached there (Malcolm et al., 2010). Other possible MeHg accumulations within oxic seawater mainly include (1) Hg methylation through anaerobic microbes in anoxic microenvironments, such as zooplankton guts, fecal pellets, and organic-rich marine particles; (2) Hg methylation through abiotic processes; and (3) Hg methylation through aerobic microbes (Wang et al., 2021).

Polar marine ecosystems are sensitive to mercury exposure, and monitoring during the past four decades showed that mercury levels detected in Arctic marine mammals, such as ringed seals, polar bears and beluga whales, have been significantly elevated over the past 150 years and frequently exceeded toxicity thresholds (Dietz et al., 2013; Wang et al., 2018). Similarly, Antarctic biota are also vulnerable to mercury exposure, and mercury biomagnification has been found in the Southern Ocean, with significantly higher Hg levels in seabirds than in zooplankton (Seco et al., 2021). One observational study in the western Antarctic Peninsula found significantly higher total Hg and MeHg levels in juvenile than adult krill, implying that krill-dependent predators, which mainly feed on juveniles, may accumulate more MeHg than consumers foraging on older krill (Sontag et al., 2019). It should be mentioned that the MeHg content and spatial distribution in seawater play an important role in the biotic MeHg level. For instance, Wang et al. (2018) suggested that the subsurface MeHg maximum can lie within the habitat of zooplankton and other lower trophic-level biota, and biological uptake of subsurface MeHg and subsequent biomagnification would explain the biotic Hg concentration gradient across the Canadian Arctic.

The measurement and analysis of MeHg levels in water is an important step to evaluate the corresponding Hg exposure risk to organisms in aquatic environments. However, due to accessibility, there have been few studies in the Southern Ocean. Cossa et al. (2011) reported the first Hg speciation measurements in the water column of the Southern Ocean from South Australia to coastal Antarctica (44–66°S). Subsequently, Nerentorp Mastromonaco et al. (2017) presented the Hg speciation concentrations and distributions in higher latitude Antarctic marginal seas. Overall, the geographical variations and corresponding influencing mechanisms of Hg methylation in the Southern Ocean still need further study.

In this study, we investigate the vertical distribution and the corresponding influencing factors of the total concentration of MeHg (the sum of monomethylmercury and dimethylmercury) in unfiltered seawater (MeHg_T , including both dissolved and particle-bound MeHg in seawater) in the high-latitude Ross and Amundsen Seas, which are home to large populations of birdlife (e.g., nearly 33 % of the world's Adelie penguin population and 30 % of the world's Antarctic petrels inhabit the Ross Sea) (Lynch and LaRue, 2015). Our objectives are to improve the understanding of the concentration, distribution, and biogeochemistry of MeHg in the Southern Ocean and to provide critical data support for further assessment of mercury exposure risk in Antarctic marine ecosystems.

2. Materials and methods

2.1. Study area

As part of the 36th Chinese National Antarctic Research Expedition (CHINARE-36th) aboard the icebreaker R/V Xuelong, seawater samples were collected at 7 CTD/rosette stations in the Antarctic Ross Sea (with 3 stations) and Amundsen Sea (with 4 stations) from 11 to 30 January 2020, with a latitude range of 67°S–74°S and a longitude range of 119°W–150°W. The corresponding sampling locations are displayed in Fig. S1.

2.2. Seawater sampling

Different depths of the water column were sampled using a rosette water sampler (Seabird, SBE32) with 24 Teflon-coated Niskin-X bottles (12 L, General Oceanics). Similar methods have been widely utilized in seawater sampling for mercury species measurements (Bratkic et al., 2016; Kim et al., 2017; Nerentorp Mastromonaco et al., 2017; Wang et al., 2012). After collection, the unfiltered seawater samples were stored in precleaned Teflon bottles with 0.4 % (v/v) double-distilled hydrochloric acid (HCl) added for Hg analysis. The bottles were then double-bagged and stored in the dark in a refrigerator at 4 °C.

2.3. MeHg_T measurements

Due to the low volume of each collected seawater sample (<300 mL) and the method used in this study, we did not measure the total Hg concentration in seawater; instead, this study focuses on the MeHg_T concentration in seawater. For the analysis of MeHg_T , 2.5 mL sulfuric acid (H_2SO_4) (1 %) was added to 250 mL unfiltered seawater samples to digest for 12 h. Following digestion, the samples were first neutralized with 3.75 mL of 50 % potassium hydroxide (KOH) and then buffered to a pH of 5 using 3 mL of a 2 M acetic acid buffer. This was followed by a 15 min ethyl-derivatization reaction after the addition of 150 μL sodium tetraethyl borate (NaBEt_4), and then the solution was purged at 300 mL/min of N_2 flow for 15 min to trap the formed methyl-ethylmercury ($\text{CH}_3\text{CH}_2\text{HgCH}_3$) on a Tenax-TA trap (35/60 mesh, Supelco, Bellefonte, PA, USA). After that, the methyl-ethylmercury on the Tenax-TA trap was thermally desorbed at 200 °C, separated through an OV-3 column at 70 °C, decomposed to Hg^0 at 800 °C, and measured using a Model III AFS (Brooks Rand Lab., Seattle, WA, USA) (Agather et al., 2019; Bowman and Hammerschmidt, 2011; Munson et al., 2014). For each set of 20 seawater samples, procedures of two method blanks, two matrix spikes (methylmercury chloride, MeHgCl) for the recovery test, and triplicates of one sample for relative standard deviation analysis were conducted. The set spike mass/concentration of MeHg_T for the recovery test of seawater samples was 0.1 ng/L. The corresponding detection limit was 0.002 ng/L, as determined by calculating three times the standard deviation of five blank replicate samples. Both the recoveries (85–104 %, $N = 8$) and relative standard deviations (1.2–8.2 %, $N = 4$) were acceptable for MeHg_T measurements (Liu et al., 2020).

2.4. Ancillary oceanographic data

Additional oceanographic data, including water temperature, salinity, dissolved oxygen (DO) and chlorophyll fluorescence (Flu), were collected with an SBE 911 plus CTD profiler and an attached Seapoint chlorophyll fluorometer (Sea-bird, Bellevue, WA, USA). Nutrients, including nitrate (the sum of NO_3^- and NO_2^-), silicate ($\text{Si}(\text{OH})_4$), and phosphate (PO_4^{3-}), were measured onboard using a continuous flow analyzer (Skalar San + +, Breda, Netherlands), and nitrite was measured using a spectrometric method (Zhuang et al., 2018). The apparent oxygen utilization (AOU), which is the difference between the measured dissolved oxygen concentration and its equilibrium saturation concentration in water with the same physical and chemical properties and can serve as a proxy for heterotrophic activity, was calculated based on the method introduced by Garcia and Gordon (1992). Data on the sea-ice fraction and 10-day-averaged shortwave radiation (Radiation) were extracted and averaged from the assimilated hourly meteorological data from the Goddard Earth Observing System-Forward Processing (GEOS-FP) meteorological field product, which has a horizontal resolution of $2^\circ \times 2.5^\circ$. Daily, densely gridded MODIS images (250 m) of the ice conditions in Antarctica from NASA's Terra satellite were acquired online (<http://lance-modis.eosdis.nasa.gov/imagery/subsets/?subset5BROMEX>).

2.5. Identification of the Antarctic water mass

The characteristics of the MeHg_T content within different water masses in the Ross and Amundsen Seas were investigated in this study. Various water masses in the Ross and Amundsen Seas were identified based on potential temperature, potential density, salinity, and depth data collected from CTD profiles. The main water masses from top to bottom include summer surface water (SSW, with an average depth of 7.47 ± 7.69 m), which is characterized by the lowest density; winter water (WW, with an average depth of 99.17 ± 67.12 m), which is characterized by the minimum subsurface temperature; circumpolar deep water (CDW, with an average depth of 579.32 ± 310.30 m), which is characterized by subsurface temperature maxima and high salinity; Antarctic bottom water (AABW, with an average depth of 4168.14 ± 289.94 m), which is the densest water mass near the bottom of the sea; and other (with an average depth of 1985.32 ± 1426.27 m), which has oceanographic properties that do not meet the core properties of any of the aforementioned main water masses. The detailed identifying methods and corresponding T-S diagrams are mainly based on Walker et al. (2013) and Whitworth et al. (1998) and presented in the Supporting Information.

2.6. Evaluation of the importance of MeHg uptake by phytoplankton

In this study, we used the Massachusetts Institute of Technology general circulation model (MITgcm) to preliminarily evaluate the contribution of phytoplankton uptake to the total MeHg mass in Antarctic surface seawater (Marshall et al., 1997). This model has included river discharge, air-sea exchange, sinking of particle MeHg, redox reactions, methylation, demethylation, and trophic transfer of MeHg in marine plankton food webs (Zhang et al., 2020). This model is coupled with an ocean plankton ecology and biogeochemistry model to simulate production and growth of different plankton species, suspended particulate matter and labile dissolved organic matters concentrations in the marine water column (Zhang et al., 2020). An established dataset of recalcitrant dissolved organic carbon (DOC) is archived into the model (Schartup et al., 2018). The ocean circulation data are provided by the nonlinear inverse modeling framework ECCO v4 (Forget et al., 2015). The resolution of the model is $1^\circ \times 1^\circ$ horizontally with 50 vertical levels.

In the MIT-gcm model, phytoplankton accumulates MeHg primarily through passive uptake from seawater (diffusion) across the cell membrane:

$$\text{MMHg}_{\text{phy}} = \text{VCF}(d, [\text{DOC}]) \times \text{MMHg}_{\text{sea}}$$

where MMHg_{phy} and MMHg_{sea} are the MMHg concentrations in phytoplankton and seawater, respectively. The volume concentration factor (VCF) is a function of the cell diameter (d , μm) and total (labile and recalcitrant) dissolved organic carbon (DOC, μM) concentrations in the model (Schartup et al., 2018):

$$\text{VCF} = 2.8 \times 10^6 \times \frac{1}{d} \times e^{-0.008\text{DOC}}$$

More details of this method can be found in Wu et al. (2020) and Schartup et al. (2018).

3. Results and discussion

3.1. Concentrations of MeHg_T in the Ross and Amundsen Seas

The concentrations of MeHg_T in the Ross and Amundsen Seas ranged from 0.015 to 0.45 pmol/L, with an average of 0.13 ± 0.11 pmol/L ($n = 64$). This is similar to those measured during the summertime of 2010/2011 in this region (0.14 ± 0.19 pmol/L) (Nerentorp Mastromonaco et al., 2017). However, the MeHg_T level in this study is lower than the results reported by Cossa et al. (2011) (0.02–0.86 pmol/L, with an average of 0.29 ± 0.21 pmol/L) obtained in the middle latitudes of the Southern Ocean (approximately 44–66°S). They especially observed high levels from the Antarctic Zone to the Southern Zone (approximately 60°S to 65°S), where the MeHg_T level below the subsurface layer (approximately 300 m depth) was generally larger than 0.5 pmol/L and was mainly attributed to in situ methylation of Hg facilitated by heterotrophic activity (Cossa et al., 2011). This might imply large differences in the capacity for Hg methylation in the Southern Ocean. The MeHg_T level measured in this study is similar to that measured in the Arctic Ocean, e.g., the Arctic Beaufort Sea (average: 0.20 ± 0.15 pmol/L; range: <0.04 to 0.59 pmol/L) and Canadian Arctic (average: 0.23 ± 0.12 pmol/L; range: 0.02 to 0.56 pmol/L) (Wang et al., 2012; Wang et al., 2018).

3.2. Vertical distribution of MeHg_T

The depth profiles of MeHg_T at the seven stations display a nearly "C" shape, with high concentration levels of MeHg_T occurring in the top 500 m and near the bottom (Fig. 1). Several previous studies found similar features (Bratkič et al., 2016; Nerentorp Mastromonaco et al., 2017). It has been widely reported that the large fluctuation of MeHg_T in the upper ocean layer (0–500 m) is driven by atmospheric Hg(II) deposition, which provides Hg substrates for methylation and the remineralization of organic matter secreted by upper marine organisms (Durnford and Dastoor, 2011; Wang et al., 2012). For the bottom ocean, the increased MeHg_T above the ocean floor (Figs. 1 and 2, with <15 m of distance from the deepest samples of stations A3–9 and A3–10 to the bottom) may be related to benthic diffusion and the resuspension of MeHg from marine sediments (Hammerschmidt et al., 2004; Hollweg et al., 2010; Kim et al., 2020). From the upper layer to the bottom (approximately 500 m–4000 m depth), the measured MeHg_T concentrations were relatively constant, which was similar to the vertical distribution characteristics in Cossa et al. (2011) and Nerentorp Mastromonaco et al. (2017), except for two fluctuating data points at approximately 1000 m and 3000 m depth, respectively. It is worth noting that Bratkič et al. (2016) measured the increasing concentrations of surface MeHg_T near the land (Gough Island) and suggested the local stimulating influence on MeHg_T formation from land (e.g., Fe input from the island, which induces phytoplankton growth and subsequently OM remineralization). However, in this study, the MeHg_T concentrations measured in the vicinity of the Antarctic continent are generally low, suggesting that the influencing scope of MeHg inputs from Antarctic shelf sediments would be limited, which may be to some extent

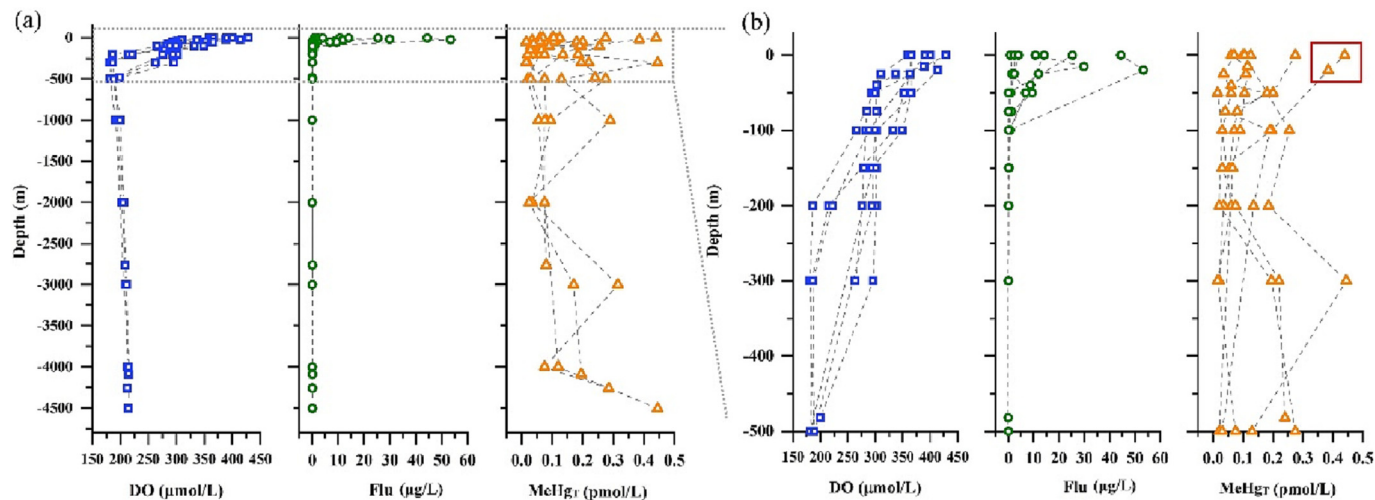


Fig. 1. Vertical profiles of total methylmercury (MeHg_T), dissolved oxygen (DO) and chlorophyll fluorescence (Flu) sampled at 7 stations in the (a) whole water column and (b) the upper 500 m depth in the Ross Sea and Amundsen Sea. The red box marks the high concentration values of MeHg_T (0.44 and 0.39 pmol/L) measured in the upper 50 m surface seawater. The corresponding vertical profiles of these parameters at each station are also displayed in the supporting information (Fig. S4).

related to the distance from the land (the nearest station (A3–10) is approximately 90 km away from the Antarctic continent).

In the subsurface ocean, heterotrophic activity associated with in situ microbial methylation is considered an important factor impacting the MeHg level (Lehnherr et al., 2011; Regnell and Watras, 2019; Wang et al., 2012). For the Southern Ocean, at latitudes of approximately 44–66°S, Cossa et al. (2011) reported a similar spatial distribution pattern between MeHg_T and AOU levels along the seawater column with a statistically significant correlation between them ($R^2 = 0.722$, $p < 0.001$). This indicates the important role of bacterial Hg methylation within the low oxygen sections of the water column (Cossa et al., 2011). In this study, a comparison between the vertical distributions of MeHg_T and AOU shows that some high values of MeHg_T can match the high AOU levels at some depths of 100–1000 m (see the black box areas in Fig. 2). This finding reflects the in-situ methylation mechanisms driven by the active heterotrophic activity in these places. However, the overall relationship between MeHg_T and AOU for all the samples is not clear (Table 1), similar to the Arctic Ocean (Agather et al., 2019), which may indicate that in situ methylation mechanisms driven by active heterotrophic activity should not be the controlling factors of MeHg_T throughout the whole water column in this study. A likely cause is the lack of an oxygen minimum zone that can offer anaerobic environments for methylating bacteria, as evidenced by the generally high DO content among the vertical profiles (180.89–428.74 $\mu\text{mol/L}$, Fig. 1).

3.3. Water mass distribution of MeHg_T

Fig. 3 shows the measured MeHg_T concentrations in different water masses. We found high MeHg_T concentrations in the SSW, contradicting many previous studies (Cossa et al., 2011; Nerentorp Mastromonaco et al., 2017). The average MeHg_T in SSW is 0.16 ± 0.12 pmol/L with a median of 0.11 pmol/L, $n = 9$, which is slightly higher than those in WW (average: 0.12 ± 0.094 pmol/L, median: 0.078 pmol/L, $n = 22$) and CDW (average: 0.135 ± 0.14 pmol/L, median: 0.075 pmol/L, $n = 16$). Interestingly, these water samples also had lower DO (WW: 310.59 ± 33.27 $\mu\text{mol/L}$, $n = 22$; CDW: 191.07 ± 8.82 $\mu\text{mol/L}$, $n = 16$) than SSW (381.75 ± 27.57 $\mu\text{mol/L}$). Moreover, in this study, the average MeHg_T concentration in SSW is approximately three times greater than that in AASW (Antarctic Surface Water) of the same sea area (0.052 ± 0.022 pmol/L) reported in Nerentorp Mastromonaco et al. (2017) and approximately 4–6 times greater than that in AASW of the Antarctic Weddell Sea (Winter: 0.039 ± 0.011 pmol/L; Spring: 0.028 ± 0.009 pmol/L) (Nerentorp Mastromonaco et al., 2017). These characteristics suggest that some

mechanisms can facilitate the large increase in MeHg_T concentrations in SSW, which will be further discussed later.

The differences between MeHg_T levels in WW and CDW were not significant ($p > 0.05$), with similar upper and lower quartile ranges. The MeHg_T level in AABW (average: 0.25 ± 0.17 pmol/L, $n = 3$) is lower than that in the same water mass measured in the 44–66°S area of the Southern Ocean (0.52 ± 0.11 pmol/L) (Cossa et al., 2011), which reflects the latitudinal difference in MeHg_T content in AABW. In addition, this concentration level is higher than that of other water masses and may be attributed to sediment resuspension/releases and/or the (re)mineralization and methylation of particulate mercury associated with the nepheloid layer here (Agather et al., 2019; Bratkič et al., 2016).

3.4. High MeHg_T in the surface ocean

The MeHg_T concentration levels in surface water reported in previous studies were usually low, with high values mainly observed in the low oxygen zones of the subsurface layer (300–500 m) (Bowman et al., 2015; Canario et al., 2017; Hammerschmidt and Bowman, 2012). In contrast, high levels of MeHg_T were also found in the surface layer (0 to 50 m, Fig. 1b) in this study, with the maximum being up to 0.44 pmol/L (at a depth of 3.35 m). This is apparently higher than the MeHg_T level in the surface water of the Arctic Ocean (<0.05 pmol/L) and the North Pacific Ocean (<0.034 pmol/L; 0 to 20 m) and the equatorial Pacific (<0.117 pmol/L; 0 to 100 m) (Heimbürger et al., 2015; Kim et al., 2017). The several high concentration values of MeHg_T observed in the surface layer were also the main cause of the elevated average concentration of MeHg_T in the SSW compared with the other water masses (see Section 3.3). A similar phenomenon was also found in the Antarctic Amundsen Sea in a previous study, with obviously higher MeHg_T levels observed in the surface seawater (Stations 14 and 31, with the corresponding measured MeHg_T exceeding 0.75 pmol/L) than in the lower water body (Mastromonaco et al., 2017). We investigated the plausible causes as follows.

3.4.1. Impact of phytoplankton mass and sea-ice

We found a significant positive correlation between MeHg_T and chlorophyll fluorescence (Flu) ($R^2 = 0.77$, $p < 0.01$) in the surface layer (0 to 50 m depth) (see Fig. 4). Due to the intrusion of nutrient-rich CDW and high Fe concentrations in glacial meltwater and in deep waters above Antarctic sediments, the Ross and Amundsen Seas are highly productive areas of the Southern Ocean (Arrigo et al., 2008; Smith and Comiso, 2008). The correlation between MeHg_T and Flu indicates phytoplankton mass as a factor that affects the distribution and accumulation of MeHg_T .

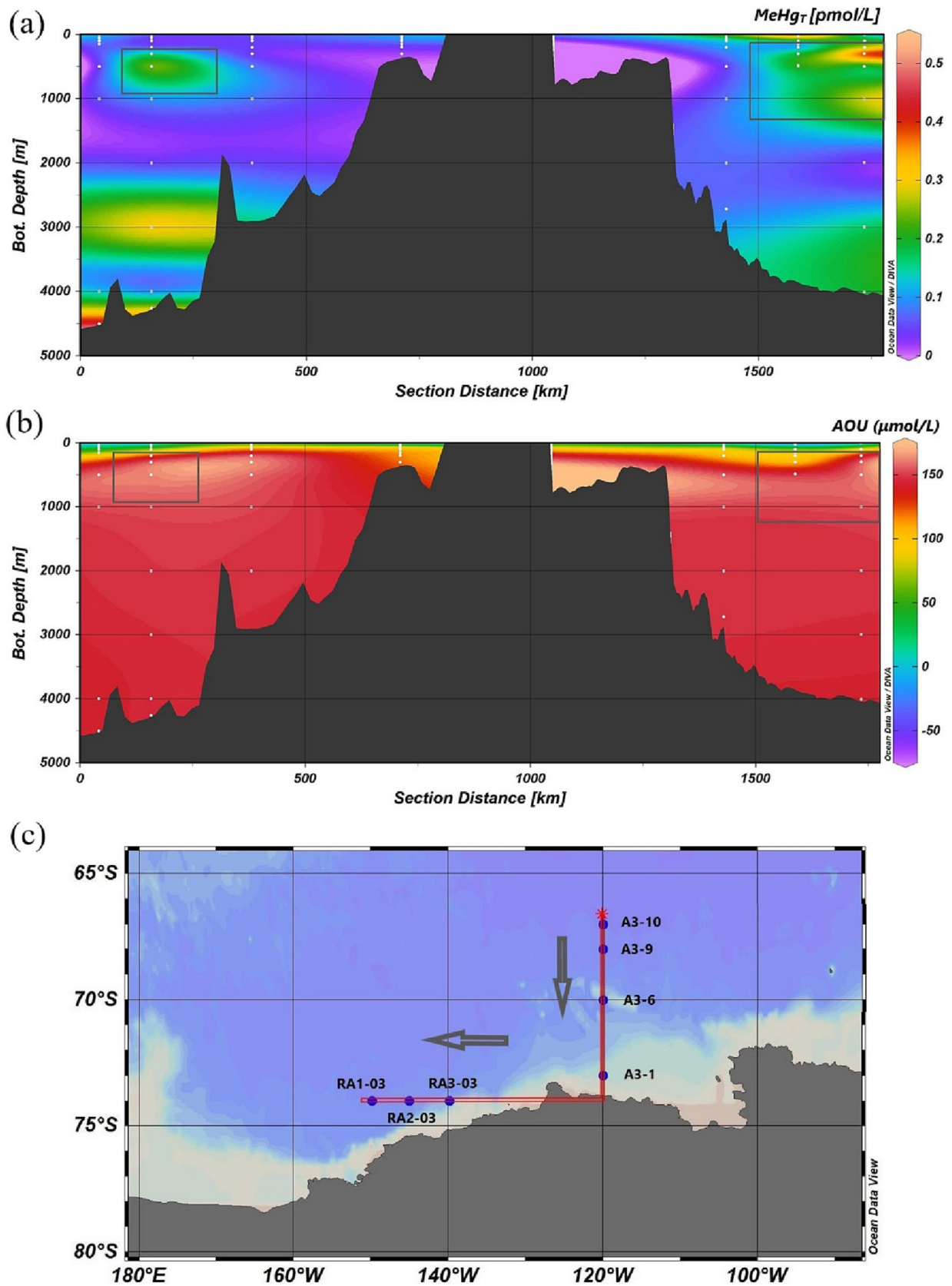


Fig. 2. Distribution of (a) total methylmercury (MeHg_T) and (b) apparent oxygen utilization (AOU) in the Ross Sea and Amundsen Sea during this cruise (CHINARE-36th). White dots indicate sampling depths, and the corresponding transect is displayed in (c), in which the black arrows indicate that the displayed transect starts with station A3-10 and ends with station RA1-3. The black boxes in (a) and (b) mark relatively high values of MeHg_T and AOUs in the subsurface layer.

Table 1

Pearson's correlation coefficients between total methylmercury (MeHg_T) and various environmental factors (NO₃⁻, PO₄³⁻, Si(OH)₄, chlorophyll fluorescence (Flu), dissolved oxygen (DO), apparent oxygen utilization (AOU), water temperature (Temp), salinity (Sal)) in different water masses (circumpolar deep water (CDW); summer surface water (SSW); winter water (WW); other water masses (Other)) in the Ross Sea and Amundsen Sea. No. in the table indicates the number of samples in each water mass.

Water mass		NO ₃ ⁻	PO ₄ ³⁻	Si(OH) ₄	Flu	DO	AOU	Temp	Sal	No.
SSW	MeHg _T	-0.20	0.064	0.63*	0.82**	0.51	-0.44	-0.24	0.43	9
WW		-0.099	-0.095	0.44*	0.6**	0.33	-0.34	0.18	-0.27	22
CDW		-0.42	-0.54*	-0.33	-0.33	-0.14	0.19	0.010	0.037	16
Other		0.32	0.26	0.10	-0.24	-0.31	0.30	0.32	0.33	13

* means the correlation is significant with p value < 0.05, and ** means the correlation is significant with p value < 0.01. Bold in the table means the corresponding correlation coefficient > 0.5 and p value < 0.05.

in surface seawater. Indeed, surface water MeHg_T concentrations vary by more than an order of magnitude in the Ross and Amundsen Seas (from 0.015 to 0.44 pmol/L). Since there is no evidence that phytoplankton can directly methylate Hg in seawater (Regnell and Watras, 2019), possible mechanisms for the association between phytoplankton biomass and MeHg_T include (1) the uptake of MeHg by phytoplankton (Wang et al., 2018), which would impact the spatial distribution of seawater total MeHg_T and result in its localized enrichment, and (2) in situ methylation, driven by the organic matter excreted from phytoplankton, which offers organic carbon that can be the anoxic microenvironment for Hg methylation by microorganisms (Gallorini and Loizeau, 2021; Heimbürger et al., 2015).

Considering that seawater samples collected in this study were not filtered, some microalgae may exist in the water samples. Marine phytoplankton can accumulate MeHg through passive diffusion from seawater across the cell membrane, resulting in concentrations of MeHg in phytoplankton being 10⁵–10⁶ times higher than those in seawater (Lee and Fisher, 2016; Schartup et al., 2018). In addition to passive uptake of MeHg, a few studies have shown that active uptake of MeHg by phytoplankton, which would be associated with energy consumption and metabolic control processes of algae cells, could also occur in some freshwater and marine phytoplankton species (Lee and Fisher, 2016; Pickhardt and Fisher, 2007; Zhong and Wang, 2009).

We further evaluated whether phytoplankton uptake can potentially affect the MeHg_T concentration in the surface seawater using MIT-gcm model simulation methods (details can be found in Section 2.6). The results showed that the calculated mass fraction of MeHg (monthly averaged)

accumulated in phytoplankton among the total MeHg mass in surface seawater (the sum of MeHg mass in phytoplankton and seawater) in the upper 50 m layer in our study area (120–150°W, 67–74°S) was 16.32 %. This fraction of MeHg bioenriched in phytoplankton may be higher if the influence of the potential active uptake of MeHg by phytoplankton is further considered. For example, Pickhardt and Fisher (2007) found that the VCF of MeHg could be 1.5– 5 times greater in living cells than in heat-killed cells of freshwater phytoplankton. However, even if we considered the impact of active uptake (with the bioenriched fraction being up to approximately 24 %–80 %), phytoplankton uptake of MeHg would not fully explain the high level of MeHg_T that we observed in the surface water of the Ross Sea and Amundsen Sea.

There is growing evidence that methylation can indeed occur in oxic water. Lehnherr et al. (2011) conducted several incubations with marine water samples from across the Canadian Arctic Archipelago. They reported that Hg methylation can occur in the oxic water column around the Chl_a maximum. Villar et al. (2020) showed metagenomic and metatranscriptomic evidence that methylation genes associated with nitrite-oxidizing bacteria (*Nitrospina*) for microbial methylmercury production are widespread in oxic seawater. The presence of anoxic microenvironments along the water column, such as particulate organic carbon (POC), can sustain Hg methylation by microorganisms, which is supported by an increasing number of reports in marine environments (Cossa et al., 2011; Gallorini and Loizeau, 2021; Heimbürger et al., 2015; Lehnherr et al., 2011). Therefore, in situ methylation facilitated by phytoplankton is definitely a possible cause for the elevated MeHg_T

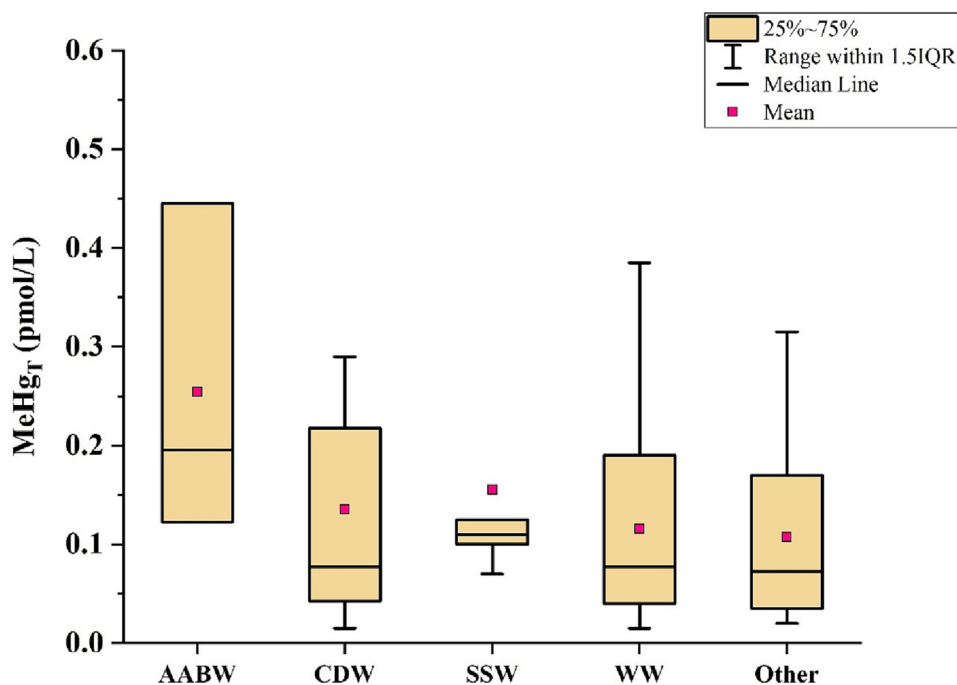


Fig. 3. Box plots of total methylmercury (MeHg_T) concentrations in various water masses (Antarctic Bottom Water (AABW, $n = 3$); Circumpolar Deep Water (CDW, $n = 16$); Summer Surface Water (SSW, $n = 9$); Winter Water (WW, $n = 22$); Other water masses (Other, $n = 13$)) in the Ross Sea and Amundsen Sea.

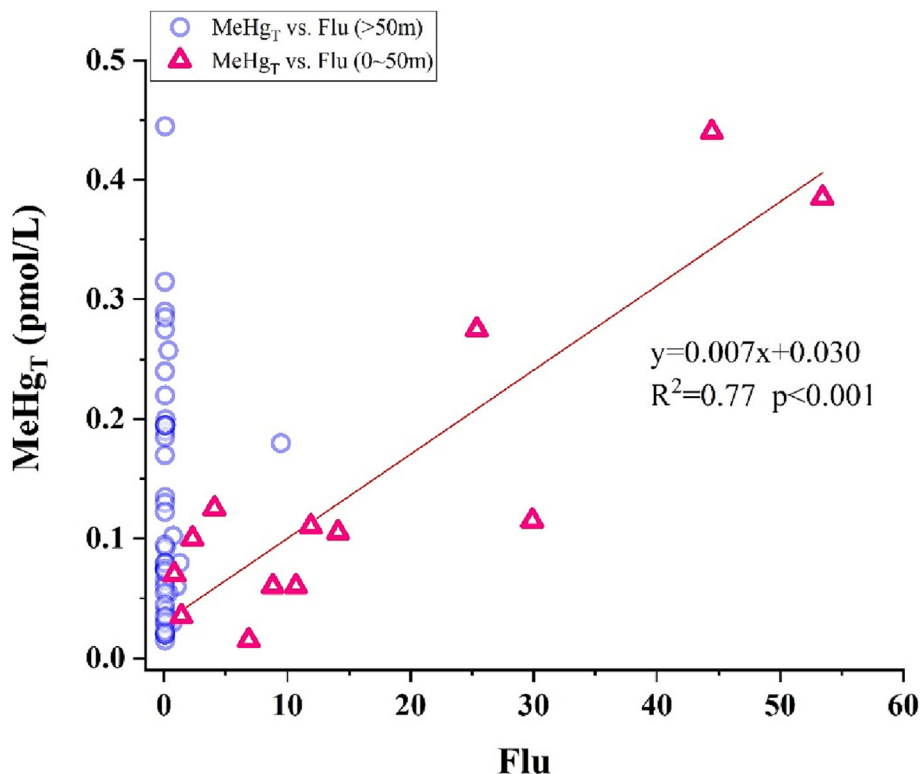


Fig. 4. Relationship between total methylmercury (MeHg_T) and chlorophyll fluorescence (Flu) in the upper 50 m depth of the Ross Sea and Amundsen Sea.

that we observed in the oxic surface layer, as high phytoplankton mass can produce more organic materials, which can be the main candidate for this ecological niche of methylating microorganisms (Gallorini and Loizeau, 2021; Heimbürger et al., 2015). Moreover, it is worth noting that we found a significant positive correlation between the average MeHg_T concentrations of the surface layer (upper 50 m) and the corresponding hourly sea-ice fractions (Fig. 5a). For example, station RA2-03, which had the highest sea-ice fraction nearby, as illustrated by the intraday satellite imagery (a large area of floating sea ice nearby, Fig. 5b), also had the highest level of MeHg_T in the surface layer. This finding indicated that sea-ice may also facilitate the elevation of MeHg_T in the surface layer of polar oceans. Gionfriddo et al. (2016) observed elevated MeHg_T in Antarctic sea-ice enriched in phytoplankton and attributed it to net microbial Hg methylation within sea ice driven by microaerophilic bacteria, such as *Nitrospina*, associated with trapped and decaying organic matter linked to the presence of bacterioplankton and phytoplankton communities. Therefore, our observed high MeHg_T level in Antarctic surface seawater could also indeed come from Hg methylation in sea-ice. This process may be further facilitated by halogen photooxidation of atmospheric Hg(0) at the sea-ice interface, which can offer more Hg(II) substrates for methylation (Dastoor et al., 2022; Durnford and Dastoor, 2011). In addition, sea-ice can trigger increased plankton mass, facilitating the production of the microenvironment (i.e., POC) that is conducive to Hg in-situ methylation in oxic water columns (Arrigo, 2014; Arrigo et al., 1997; Deppeler and Davidson, 2017). These characteristics were also reflected in our data: the surface (upper 50 m) average Flu was significantly positively correlated with sea-ice fractions ($R^2 = 0.75$, $p < 0.01$, Fig. S5), and the highest MeHg_T level was found at station RA2-03, which also had the highest sea-ice fraction and flu levels (Fig. 5a). In summary, we speculated that in-situ methylation of Hg facilitated by elevated phytoplankton mass and the presence of sea-ice might play an important role in the observed high level of MeHg_T in Antarctic oxic surface seawater.

Baya et al. (2015) observed a low concentration level of DMHg in surface seawater (3.4 ± 1.96 pg/L– 6.8 ± 6.0 pg/L) and a high mass fraction

of DMHg among total MeHg (with a mass ratio of DMHg/MMHg larger than 1) in the subsurface chlorophyll maximum in the Canadian Arctic Archipelago. In addition, this study found that the primary production rate and sea-ice cover displayed significant correlations with the DMHg concentration in the Arctic marine boundary layer, indicating their important influences on the MeHg cycle in the polar area. As we have not separately measured MMHg and DMHg, we proposed that more corresponding measurements are needed to better understand the MeHg species characteristics and their cycling processes in Antarctic marine areas, especially in sea-ice regions with high phytoplankton masses.

3.4.2. Impact of solar radiation

The MeHg content in surface seawater is also affected by demethylation processes, especially photodemethylation, which is driven by solar radiation. Zhang et al. (2020) suggested that the weaker photodemethylation in the Southern Ocean (driven by lower solar radiation and higher chlorophyll content) leads to a higher MeHg concentration in the surface seawater than in the middle- and low-latitude seas, although the latter two areas have higher methylation rates. However, we found no significant negative relationship between the average MeHg_T concentrations of the upper 50 m of every sampling station (the euphotic zone depth is ~40 m in polar summertime, Wang et al., 2012) and their corresponding 10-day-averaged solar radiation. We also found that the higher MeHg_T contents generally corresponded with higher chlorophyll levels, where their corresponding solar radiations were higher (Fig. 5c). We thus speculate that the higher chlorophyll content can attenuate solar radiation in water and weaken photodemethylation (e.g., the RA2-03 and RA3-03 stations, Fig. 5c).

4. Conclusions

Previous studies have shown that spatial variation in MeHg concentrations within the subsurface zone has an important influence on the distribution of biotic Hg levels in the Arctic Ocean (Wang et al., 2018). In this study, we report elevated MeHg_T in Antarctic surface seawater and postulate that the enrichment may be driven by the increased phytoplankton mass and the

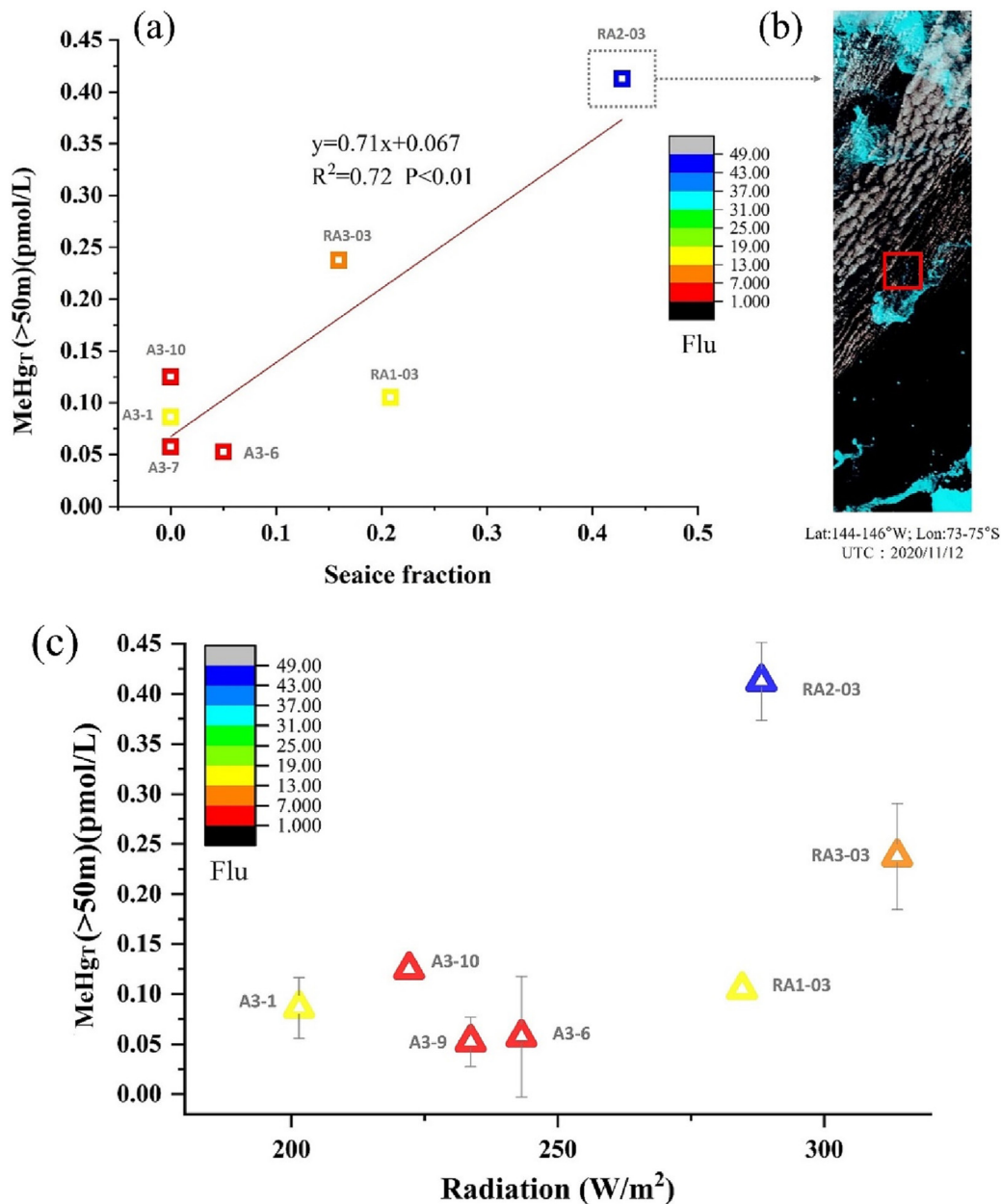


Fig. 5. Relationship between total methylmercury (MeHg_T) in the upper 50 m depth of unfiltered seawater and (a) sea-ice fraction and (c) 10-day averaged shortwave radiation (radiation). The color bar in each figure represents the average chlorophyll fluorescence (Flu, µg/L) of each station. The red box in the satellite imagery (b) marks the location of station RA2-03, which displays a large area of floating sea ice nearby. The area with blue color in this figure represents the sea ice cover area.

presence of sea-ice, which can facilitate MeHg in-situ methylation and algae uptake and then result in the localized enrichment of MeHg_T in surface seawater. As the surface layer of the Southern Ocean is the major feeding ground for higher organisms (e.g., penguins, seals, seabirds, etc.) in summertime, the produced MeHg incorporated into phytoplankton is likely to impact Hg biomagnification and exposure in susceptible Antarctic ecosystems. Further studies are needed to evaluate the ecological effects. In addition, we need to acknowledge that the interpretation in this study is to some extent limited by the lack of contextual total Hg data, and more studies are still needed to further investigate the source of MeHg in oxic seawater.

CRedit authorship contribution statement

1. Fange Yue: Roles/Writing - original draft; Investigation; Formal analysis; Methodology
2. Yanbin Li: Methodology; Resources; Investigation

3. Yanxu Zhang: Writing - review & editing; Investigation
4. Longquan Wang: Resources
5. Dan Li: Methodology
6. Peipei Wu: Investigation
7. Hongwei Liu: Investigation
8. Lijin Lin: Methodology
9. Dong Li: Resources
10. Ji Hu: Resources
11. Zhouqing Xie: Conceptualization; Data curation; Funding acquisition; Investigation; Project administration; Resources; Supervision

Data availability

The data are available at <https://data.mendeley.com/datasets/x7r6mprjb7/1>.

Declaration of competing interest

The authors declare that they have no known competing financial interests or personal relationships that could have appeared to influence the work reported in this paper.

Acknowledgments

This work was supported by the National Natural Science Foundation of China (grant nos. 41941014 and 41930532) and the Ministry of Natural Resources of the People's Republic of China (IRASCC2020-2022-No. 01-01-02E and IRASCC2020-2022-No. 01-01-02A). We thank the China Arctic and Antarctic Administration for fieldwork support. We thank Mr. Guijun Guo from the First Institute of Oceanography, Ministry of Natural Resources, for providing the oceanographic data. We thank Dr. Zhengbing Han, Prof. Jianming Pan and Dr. Jun Zhao from the Second Institute of Oceanography, Ministry of Natural Resources for helpful discussion.

Appendix A. Supplementary data

Supplementary data to this article can be found online at <https://doi.org/10.1016/j.scitotenv.2023.163646>.

References

- Agather, A.M., Bowman, K.L., Lamborg, C.H., Hammerschmidt, C.R., 2019. Distribution of mercury species in the Western Arctic Ocean (U.S. GEOTRACES GN01). *Mar. Chem.* 216, 103686. <https://doi.org/10.1016/j.marchem.2019.103686>.
- Andreoli, V., Sprovieri, F., 2017. Genetic aspects of susceptibility to mercury toxicity: an overview. *Int. J. Environ. Res. Public Health* 14. <https://doi.org/10.3390/ijerph14010093>.
- Ariya, P.A., Amyot, M., Dastoor, A., Deeds, D., Feinberg, A., Kos, G., Poulain, A., Ryzkov, A., Semeniuk, K., Subir, M., Toyota, K., 2015. Mercury physicochemical and biogeochemical transformation in the atmosphere and at atmospheric interfaces: a review and future directions. *Chem. Rev.* 115, 3760–3802. <https://doi.org/10.1021/cr500667e>.
- Arrigo, K.R., 2014. Sea ice ecosystems. *Annu. Rev. Mar. Sci.* 6, 439–467. <https://doi.org/10.1146/annurev-marine-010213-135103>.
- Arrigo, K.R., van Dijken, G.L., Bushinsky, S., 2008. Primary production in the Southern Ocean, 1997–2006. *J. Geophys. Res. Oceans* 113. <https://doi.org/10.1029/2007JC004551>.
- Arrigo, K.R., Worthen, D.L., Lizotte, M.P., Dixon, P., Dieckmann, G., 1997. Primary production in Antarctic Sea ice. *Science* 276, 394–397. <https://doi.org/10.1126/science.276.5311.394>.
- Baya, P.A., Gosselin, M., Lehnher, I., St.Louis, V.L., Hintelmann, H., 2015. Determination of monomethylmercury and dimethylmercury in the Arctic marine boundary layer. *Environ. Sci. Technol.* 49, 223–232. <https://doi.org/10.1021/es502601z>.
- Beckers, F., Rinklebe, J., 2017. Cycling of mercury in the environment: sources, fate, and human health implications: a review. *Crit. Rev. Environ. Sci. Technol.* 47, 693–794. <https://doi.org/10.1080/10643389.2017.1326277>.
- Bowman, K.L., Hammerschmidt, C.R., 2011. Extraction of monomethylmercury from seawater for low-femtomolar determination. *Limnol. Oceanogr. Methods* 9, 121–128. <https://doi.org/10.4319/lom.2011.9.121>.
- Bowman, K.L., Hammerschmidt, C.R., Lamborg, C.H., Swarr, G., 2015. Mercury in the North Atlantic Ocean: the U.S. GEOTRACES zonal and meridional sections. *Deep-Sea Res. II Top. Stud. Oceanogr.* 116, 251–261. <https://doi.org/10.1016/j.dsr2.2014.07.004>.
- Bratkić, A., Vahčić, M., Kotnik, J., Obu Vazner, K., Begu, E., Woodward, E.M.S., Horvat, M., 2016. Mercury presence and speciation in the South Atlantic Ocean along the 40°S transect. *Glob. Biogeochem. Cycles* 30, 105–119. <https://doi.org/10.1002/2015GB005275>.
- Canario, J., Santos-Echeandia, J., Padeiro, A., Amaro, E., Strass, V., Klaas, C., Hoppema, M., Ossebaer, S., Koch, B.P., Laglera, L.M., 2017. Mercury and methylmercury in the Atlantic sector of the Southern Ocean. *Deep-Sea Res. II Top. Stud. Oceanogr.* 138, 52–62. <https://doi.org/10.1016/j.dsr2.2016.07.012>.
- Clarkson, T.W., Magos, L., 2006. The toxicology of mercury and its chemical compounds. *Crit. Rev. Toxicol.* 36, 609–662. <https://doi.org/10.1080/10408440600845619>.
- Cossa, D., Heimbürger, L.-E., Lannuzel, D., Rintoul, S.R., Butler, E.C.V., Bowie, A.R., Averty, B., Watson, R.J., Remenyi, T., 2011. Mercury in the Southern Ocean. *Geochim. Cosmochim. Acta* 75, 4037–4052. <https://doi.org/10.1016/j.gca.2011.05.001>.
- Dastoor, A., Wilson, S.J., Travnikov, O., Ryzkov, A., Angot, H., Christensen, J.H., Steenhuisen, F., Muntean, M., 2022. Arctic atmospheric mercury: sources and changes. *Sci. Total Environ.* 839, 156213. <https://doi.org/10.1016/j.scitotenv.2022.156213>.
- Deppeler, S.L., Davidson, A.T., 2017. Southern Ocean phytoplankton in a changing climate. *Front. Mar. Sci.* 4. <https://doi.org/10.3389/fmars.2017.00040>.
- Dietz, R., Sonne, C., Basu, N., Braune, B., O'Hara, T., Letcher, R.J., Scheuhammer, T., Andersen, M., Andreasen, C., Andriashchek, D., Asmund, G., Aubail, A., Baagøe, H., Born, E.W., Chan, H.M., Derocher, A.E., Grandjean, P., Knott, K., Kirkegaard, M., Krey, A., Lunn, N., Messier, F., Obbard, M., Olsen, M.T., Ostertag, S., Peacock, E., Renzoni, A., Rigét, F.F., Skaare, J.U., Stern, G., Stirling, I., Taylor, M., Wiig, Ø., Wilson, S., Aars, J., 2013. What are the toxicological effects of mercury in Arctic biota? *Sci. Total Environ.* 443, 775–790. <https://doi.org/10.1016/j.scitotenv.2012.11.046>.
- Driscoll, C.T., Mason, R.P., Chan, H.M., Jacob, D.J., Pirrone, N., 2013. Mercury as a global pollutant: sources, pathways, and effects. *Environ. Sci. Technol.* 47, 4967–4983. <https://doi.org/10.1021/es305071v>.
- Durnford, D., Dastoor, A., 2011. The behavior of mercury in the cryosphere: a review of what we know from observations. *J. Geophys. Res. Atmos.* 116. <https://doi.org/10.1029/2010JD014809>.
- Forget, G., Campin, J.-M., Heimbach, P., Hill, C.N., Ponte, R.M., Wunsch, C., 2015. ECCO version 4: an integrated framework for non-linear inverse modeling and global ocean state estimation. *Geosci. Model Dev.* 8, 3071–3104.
- Gallorini, A., Loizeau, J.-L., 2021. Mercury methylation in oxic aquatic macro-environments: a review. *J. Limnol.* 80. <https://doi.org/10.4081/jlimnol.2021.2007>.
- Garcia, H.E., Gordon, L.I., 1992. Oxygen solubility in seawater - better fitting equations. *Limnol. Oceanogr.* 37, 1307–1312. <https://doi.org/10.4319/lo.1992.37.6.1307>.
- Gionfriddo, C.M., Tate, M.T., Wick, R.R., Schultz, M.B., Zemla, A., Thelen, M.P., Schofield, R., Krabbenhoft, D.P., Holt, K.E., Moreau, J.W., 2016. Microbial mercury methylation in Antarctic sea ice. *Nat. Microbiol.* 1, 16127. <https://doi.org/10.1038/nmicrobiol.2016.127>.
- Hammerschmidt, C.R., Bowman, K.L., 2012. Vertical methylmercury distribution in the subtropical North Pacific Ocean. *Mar. Chem.* 132–133, 77–82. <https://doi.org/10.1016/j.marchem.2012.02.005>.
- Hammerschmidt, C.R., Fitzgerald, W.F., Lamborg, C.H., Balcom, P.H., Visscher, P.T., 2004. Biogeochemistry of methylmercury in sediments of Long Island Sound. *Mar. Chem.* 90, 31–52. <https://doi.org/10.1016/j.marchem.2004.02.024>.
- Heimbürger, L.-E., Sonke, J.E., Cossa, D., Point, D., Lagane, C., Laffont, L., Galfond, B.T., Nicolaus, M., Rabe, B., van der Loeff, M.R., 2015. Shallow methylmercury production in the marginal sea ice zone of the central Arctic Ocean. *Sci. Rep.* 5, 10318. <https://doi.org/10.1038/srep10318>.
- Hollweg, T.A., Gilmour, C.C., Mason, R.P., 2010. Mercury and methylmercury cycling in sediments of the mid-Atlantic continental shelf and slope. *Limnol. Oceanogr.* 55, 2703–2722. <https://doi.org/10.4319/lo.2010.55.6.2703>.
- Kim, H., Soerensen, A.L., Hur, J., Heimbürger, L.-E., Hahn, D., Rhee, T.S., Noh, S., Han, S., 2017. Methylmercury mass budgets and distribution characteristics in the Western Pacific Ocean. *Environ. Sci. Technol.* 51, 1186–1194. <https://doi.org/10.1021/acs.est.6b04238>.
- Kim, J., Soerensen, A.L., Kim, M.S., Eom, S., Rhee, T.S., Jin, Y.K., Han, S., 2020. Mass budget of methylmercury in the East Siberian Sea: the importance of sediment sources. *Environ. Sci. Technol.* 54, 9949–9957. <https://doi.org/10.1021/acs.est.0C00154>.
- Lee, C.-S., Fisher, N.S., 2016. Methylmercury uptake by diverse marine phytoplankton. *Limnol. Oceanogr.* 61, 1626–1639. <https://doi.org/10.1002/lno.10318>.
- Lehnher, I., St. Louis, V.L., Hintelmann, H., Kirk, J.L., 2011. Methylation of inorganic mercury in polar marine waters. *Nat. Geosci.* 4, 298–302. <https://doi.org/10.1038/ngen01134>.
- Liu, C., Chen, L., Liang, S., Li, Y., 2020. Distribution of total mercury and methylmercury and their controlling factors in the East China Sea. *Environ. Pollut.* 258, 113667. <https://doi.org/10.1016/j.envpol.2019.113667>.
- Lynch, H.J., LaRue, M.A., 2015. Erratum: first global census of the Adélie Penguin. *Auk* 132, 562. <https://doi.org/10.1642/AUK-15-20.1> %J The Auk.
- Malcolm, E.G., Schaefer, J.K., Ekstrom, E.B., Tuit, C.B., Jayakumar, A., Park, H., Ward, B.B., Morel, F.M.M., 2010. Mercury methylation in oxygen deficient zones of the oceans: no evidence for the predominance of anaerobes. *Mar. Chem.* 122, 11–19. <https://doi.org/10.1016/j.marchem.2010.08.004>.
- Marshall, J., Adcroft, A., Hill, C., Perelman, L.T., Heisey, C., 1997. A finite-volume, incompressible navier stokes model for studies of the ocean on parallel computers. *J. Geophys. Res.* 102, 5753–5766.
- McMeans, B.C., Arts, M.T., Fisk, A.T., 2015. Impacts of food web structure and feeding behavior on mercury exposure in Greenland sharks (*Somniosus microcephalus*). *Sci. Total Environ.* 509–510, 216–225. <https://doi.org/10.1016/j.scitotenv.2014.01.128>.
- Munson, K.M., Babi, D., Lamborg, C.H., 2014. Determination of monomethylmercury from seawater with ascorbic acid-assisted direct ethylation. *Limnol. Oceanogr.-Methods* 12, 1–9. <https://doi.org/10.4319/lom.2014.12.1>.
- Nerentorp Mastrodonato, M.G., Gårdfeldt, K., Assmann, K.M., Langer, S., Delali, T., Shlyapnikov, Y.M., Zivkovic, I., Horvat, M., 2017. Speciation of mercury in the waters of the Weddell, Amundsen and Ross Seas (Southern Ocean). *Mar. Chem.* 193, 20–33. <https://doi.org/10.1016/j.marchem.2017.03.001>.
- Parks Jerry, M., Johs, A., Podar, M., Bridou, R., Hurt Richard, A., Smith Steven, D., Tomanicek Stephen, J., Qian, Y., Brown Steven, D., Brandt Craig, C., Palumbo Anthony, V., Smith Jeremy, C., Wall Judy, D., Elias Dwayne, A., Liang, L., 2013. The genetic basis for bacterial mercury methylation. *Science* 339, 1332–1335. <https://doi.org/10.1126/science.1230667>.
- Pickhardt, P.C., Fisher, N.S., 2007. Accumulation of inorganic and methylmercury by freshwater phytoplankton in two contrasting water bodies. *Environ. Sci. Technol.* 41, 125–131. <https://doi.org/10.1021/es060966w>.
- Regnell, O., Watras, C.J., 2019. Microbial mercury methylation in aquatic environments: a critical review of published field and laboratory studies. *Environ. Sci. Technol.* 53, 4–19. <https://doi.org/10.1021/acs.est.8b02709>.
- Roman Henry, A., Walsh Tyra, L., Coull Brent A., Dewailly, É., Guallar, E., Hattis, D., Mariën, K., Schwartz, J., Stern Alan, H., Virtanen Jyrki, K., Rice, G., 2011. Evaluation of the cardiovascular effects of methylmercury exposures: current evidence supports development of a dose-response function for regulatory benefits analysis. *Environ. Health Perspect.* 119, 607–614. <https://doi.org/10.1289/ehp.1003012>.
- Schartup, A.T., Qureshi, A., Dassuncao, C., Thackray, C.P., Harding, G., Sunderland, E.M., 2018. A model for methylmercury uptake and trophic transfer by marine plankton. *Environ. Sci. Technol.* 52, 654–662. <https://doi.org/10.1021/acs.est.7b03821>.
- Seco, J., Aparicio, S., Brierley, A.S., Bustamante, P., Ceia, F.R., Coelho, J.P., Philips, R.A., Saunders, R.A., Fielding, S., Gregory, S., Matias, R., Pardal, M.A., Pereira, E., Stowasser, G., Tarling, G.A., Xavier, J.C., 2021. Mercury biomagnification in a Southern Ocean food web. *Environ. Pollut.* 275, 116620. <https://doi.org/10.1016/j.envpol.2021.116620>.

- Smith Jr., W.O., Comiso, J.C., 2008. Influence of sea ice on primary production in the Southern Ocean: a satellite perspective. *J. Geophys. Res. Oceans* 113. <https://doi.org/10.1029/2007JC004251>.
- Sontag, P.T., Steinberg, D.K., Reinfelder, J.R., 2019. Patterns of total mercury and methylmercury bioaccumulation in Antarctic krill (*Euphausia superba*) along the West Antarctic Peninsula. *Sci. Total Environ.* 688, 174–183. <https://doi.org/10.1016/j.scitotenv.2019.06.176>.
- Villar, E., Cabrol, L., Heimbürger-Boavida, L.-E., 2020. Widespread microbial mercury methylation genes in the global ocean. *Environ. Microbiol. Rep.* 12, 277–287. <https://doi.org/10.1111/1758-2229.12829>.
- Walker, D.P., Jenkins, A., Assmann, K.M., Shoosmith, D.R., Brandon, M.A., 2013. Oceanographic observations at the shelf break of the Amundsen Sea, Antarctica. *J. Geophys. Res. Oceans* 118, 2906–2918. <https://doi.org/10.1002/jgrc.20212>.
- Wang, F., Macdonald, R.W., Armstrong, D.A., Stern, G.A., 2012. Total and methylated mercury in the Beaufort sea: the role of local and recent organic remineralization. *Environ. Sci. Technol.* 46, 11821–11828. <https://doi.org/10.1021/es302882d>.
- Wang, K., Liu, G., Cai, Y., 2021. Possible pathways for mercury methylation in oxic marine waters. *Crit. Rev. Environ. Sci. Technol.*, 1–19 <https://doi.org/10.1080/10643389.2021.2008753>.
- Wang, K., Munson, K.M., Beaupré-Laperrière, A., Mucci, A., Macdonald, R.W., Wang, F., 2018. Subsurface seawater methylmercury maximum explains biotic mercury concentrations in the Canadian Arctic. *Sci. Rep.* 8, 14465. <https://doi.org/10.1038/s41598-018-32760-0>.
- Whitworth, T., Orsi, A.H., Kim, S.J., Nowlin, W.D., Locarnini, R.A., 1998. Water masses and mixing near the Antarctic Slope Front. *Ocean, Ice and Atmosphere: Interactions at the Antarctic Continental Margin*. Antarctic Research Series 75. American Geophysical Union, pp. 1–27. <https://doi.org/10.1029/AR075p0001>.
- Wu, P., Kainz, M.J., Bravo, A.G., Åkerblom, S., Sonesten, L., Bishop, K., 2019. The importance of bioconcentration into the pelagic food web base for methylmercury biomagnification: a meta-analysis. *Sci. Total Environ.* 646, 357–367. <https://doi.org/10.1016/j.scitotenv.2018.07.328>.
- Wu, P., Zakem, E.J., Dutkiewicz, S., Zhang, Y., 2020. Biomagnification of methylmercury in a marine plankton ecosystem. *Environ. Sci. Technol.* 54, 5446–5455. <https://doi.org/10.1021/acs.est.9b06075>.
- Yue, F., Xie, Z., Zhang, Y., Yan, J., Zhao, S., 2022. Latitudinal distribution of gaseous elemental mercury in tropical western Pacific: the role of the doldrums and the ITCZ. *Environ. Sci. Technol.* <https://doi.org/10.1021/acs.est.1c07229>.
- Zhang, Y., Soerensen, A.L., Schartup, A.T., Sunderland, E.M., 2020. A global model for methylmercury formation and uptake at the base of marine food webs. *Glob. Biogeochem. Cycles* 34, e2019GB006348. <https://doi.org/10.1029/2019GB006348>.
- Zhong, H., Wang, W.-X., 2009. Controls of dissolved organic matter and chloride on mercury uptake by a marine diatom. *Environ. Sci. Technol.* 43, 8998–9003. <https://doi.org/10.1021/es901646k>.
- Zhuang, Y., Jin, H., Chen, J., Li, H., Ji, Z., Bai, Y., Zhang, T., 2018. Nutrient and phytoplankton dynamics driven by the Beaufort Gyre in the western Arctic Ocean during the period 2008–2014. *Deep-Sea Res. I Oceanogr. Res. Pap.* 137, 30–37. <https://doi.org/10.1016/j.dsr.2018.05.002>.